BJRS

BRAZILIAN JOURNAL
OF
RADIATION SCIENCES
10-04 (2022) 01-12

# $^{18}$F-FES radiation dosimetry preliminary estimates for preclinical studies based on voxelized phantom

Ferreira[a] A.V., Bispo[a] A.C.A., Leite[a] C.S., Silva[a] J.B., Mamede[b] M., Gontijo[b] R.M.G., Mendes[a] B.M.

[a] *Centro de Desenvolvimento da Tecnologia Nuclear, Av. Presidente Antônio Carlos, 6.627, 31270-901, Belo Horizonte, MG, Brazil*

[b] *Universidade Federal de Minas Gerais (UFMG)/ Departamento de Anatomia e Imagem, Belo Horizonte, MG, Brasil*
*avf@cdtn.br*

## ABSTRACT

**Small animals, such as mice, are used in radiopharmaceutical biodistribution studies and innumerous others preclinical investigations involving ionizing radiation. Longitudinal preclinical studies with five or more image procedures, involving radiopharmaceuticals injection and/or X-radiation, are not uncommon. However, a suitable dosimetric evaluation is not always available and, sometimes, absorbed doses in animal organs or tissues and their influence in experimental results were not appropriately taken into account. Accurate calculation of absorbed doses in mice organs are needed to evaluate potential radiobiological effects that may interfere with *in vivo* experiments. In this work, we perform a preliminary 16α-[$^{18}$F]-fluoro-17β-estradiol ($^{18}$F-FES) radiation dosimetry estimates for female mice. The obtained animal dosimetric results can be useful for evaluating animal doses during the design of longitudinal preclinical studies.**

***Keywords:*** **radiation dosimetry, $^{18}$F-FES, preclinical studies**

ISSN: 2319-0612
DOI: https://doi.org/10.15392/2319-0612.2022.2089
Submitted: 2022-07-12
Accepted: 2022-09-19

## 1. INTRODUCTION

Breast cancer is one of the most prevalent and aggressive types of cancer in women, therefore is also one of the principal causes of death by cancer worldwide [1]. With its early diagnosis and treatment, the chances of mortality or morbidity caused by the disease can significantly decrease and improve life quality for the population that is more affected by it.

This pathology may present several subtypes, which are differentiated by the expression profile of hormone receptors in tumor cells, that's why the $^{18}$F-Fludeoxyglucose ($^{18}$F-FDG), which is based on the increased glycolytic metabolism of tumor cells [2], and the most widely radiopharmaceutical used for breast cancer diagnosis, may not be the ideal radiotracer to detect this type of cancer. In this context, 16α-[$^{18}$F]-fluoro-17β-estradiol ($^{18}$F-Fluoroestradiol or $^{18}$F-FES), which is an estrogen analogue, were developed to investigate breast cancers with increased expression of estrogen receptors. The radiopharmaceutical allows the evaluation of the receptor profile of tumor cells, an important factor for determining the therapy to be used, with potential value in disease staging, prognosis and response to the therapy [3-5].

Small animals, such as mice, are used in radiopharmaceuticals biodistribution studies and innumerous others preclinical investigations involving ionizing radiation. Longitudinal preclinical studies with five or more image procedures (microCT and/or PET/SPECT) are not uncommon [6-13] Nevertheless, accurate mice dosimetry is not always available. In these cases, influence of the absorbed doses levels in experimental results could not be appropriately evaluated. Works have shown that even low doses (50 to 500 mGy) can induce biological effects in mice [14, 15]. In such cases, the precise quantification of absorbed doses in mice organs is very important to evaluate potential radiobiological effects that may interfere with *in vivo* experiments [16]. In this context, voxelized mice computational models were found to be a significant tool for animal internal dosimetry estimates [17]. These models are anatomically realistic and can be used in numerical simulations using radiation transport codes.

Considering the use of $^{18}$F-FES in longitudinal preclinical studies, the main objective of this work was to perform a preliminary $^{18}$F-FES dosimetry estimate for female mice. In this sense, $^{18}$F-FES was synthetized and injected in healthy female mice to performed biodistribution studies. Experimental biodistribution data and the FM_BRA voxelized female mouse model [18] were used in Monte Carlo

simulations in order to obtain $^{18}$F-FES radiation dose estimates. Dosimetric results can be used to support the design of longitudinal preclinical studies, avoiding unwanted animal radiation dose that that may interfere with experiment.

## 2. MATERIALS AND METHODS

### 2.1 $^{18}$F-FES *ex vivo* biodistribution and PET image in mice

$^{18}$F-FES was produced in the Radiopharmaceutical Research and Production Unit (UPPR) of the Nuclear Technology Development Center (CDTN/CNEN) according described in elsewhere [19]. Protocols used in animal studies were approved by the Ethics Committee on Animal Use (CEUA-IPEN/SP) under registration no 002/016 CEUA/IPEN/SP: 115/13. Experiments were performed in compliance with guidelines of the National Council Control in Animal Experiments (CONCEA).

Female Swiss mice were fasted for 6 h with *ad libitum* access to water before *ex vivo* biodistribution studies. $^{18}$F-FES (0.1 MBq/100 µl) was injected through the lateral tail vein of the animals (20–30 g). Five mice at each biodistribution time (5, 30, 60, 120 and 180 min after injection) were sacrificed by cervical dislocation. Blood samples were obtained by cardiac puncture. Organs and tissues samples (spleen, bladder, brain, heart, stomach, liver, small intestine, large intestine, muscle, bone, ovaries, pancreas, lungs, kidneys and uterus) were excised, washed and weighted. Organs and tissues radioactivity was measured in an automatic gamma counter [2480 WIZARD; PerkinElmer (Wallac Oy), Joensuu, Finland].

Additionally, a small animal PET scanner (LabPET4, GE healthcare Technologies, Waukesha, WI) from Molecular Imaging Laboratory (LIM) of Nuclear Technology Development Center (CDTN) was used in the $^{18}$F-FES PET images studies. Female Swiss mice were fasted for 4–6 h with *ad libitum* access to water before image acquisition. Protocols for PET imaging included an injected dose of 12-15 MBq/100 µl and isoflurane 2% as anesthesia. 15-min static acquisitions with three bed positions were performed. Images acquisition and reconstruction were performed using the LabPET 1.12.1 software, provided by the small-animal PET scanner manufacturer. After acquisition, PET images were reconstructed following the LIM/CDTN standard protocol: MLEM-3D algorithm, 20

iterations, no high-resolution mode, no attenuation or scatter corrections, no post-filtering. PET images post-processing were performed using AMIDE software [20].

**2.2 Animal Dosimetry**

Biodistribution data in mice were used to estimate absorbed doses. $^{18}$F-FES uptake values (%ID/g) were converted to percentage injected dose per organ/tissue using animal organ/tissue reference masses from FM_BRA, a female mouse computational model described elsewhere [18].

Time-activity curves for each measured organ/tissue were generated. For each curve, time-integrated activity in the source region, $\tilde{A}$ (area under the curve), formerly called cumulated activity, was determined by trapezoidal integration until 180 min after injection. After the last measured time point (180 min), it was assumed that the radiotracer underwent only physical decay with no biological elimination from the source organ.

The MIRD formulation [21] was applied to calculate the absorbed radiation dose for the animal organs/tissues:

$$\mathbf{D}\,(\mathbf{r_k}) = \sum_{\mathbf{h}} \tilde{A}_{\mathbf{h}} * \mathbf{S}(\mathbf{r_k} \leftarrow \mathbf{r_h}) \qquad \textbf{(1)}$$

where $\mathbf{D(r_k)}$ is the target organ $\mathbf{r_k}$ absorbed dose, $\tilde{\mathbf{A}}_{\mathbf{h}}$ is the cumulate activity in the source organ $\mathbf{r_h}$ and $\mathrm{S}(\mathbf{r_k} \leftarrow \mathbf{r_k})$ is the dose factor (mean absorbed dose per cumulated activity). S values for animal organs/tissues were obtained from the FM_BRA mouse voxel model. Since there were no available models for mice urinary and fecal excretion of the $^{18}$F-FES, a conservative approach was adopted: all decays of the F-18 were considered to occur inside de animal. In this case all F-18 decays that were not integrated in the organs of the biodistribution study will be distributed in the remaining (not collected) organs.

The MCNP6 (Version.1) Monte Carlo code was adopted on simulations [22]. It was installed in Windows operational system. The CPU was an Intel® Core™ i7-4790 @ 3.6 GHz and 16GB RAM. The S-value was calculated with MCNP6 as the mean absorbed dose in a target-organ per nuclear disintegration in the source-organ. The tissue composition and density of FM_BRA organs and tissues were based on ICRP 110 values reported for human organs [23]. One case was simulated for each organ of the mice model as the source-organ. In these simulations, all organs of the model (including the

source-organ) were considered as target-organs, i.e., the absorbed dose contributions for all organs of the model were evaluated for each source-organ. Positron sources uniformly distributed inside each source organ were prepared. The F-18 positron spectrum was obtained in DECDATA® software provided in ICRP 107 [24]. Photons and electrons/positrons were transported (mode p e). Therefore, 511 keV photons were generated in the positron annihilations and their histories were also followed by the code. The tally +F6 was used to estimate the mean absorbed dose ($MeV.g^{-1}$) in target-organ per particle emitted in the source. The +F6 results were converted to Gy per emitted positron. According to ICRP 107 (2008), F-18 emits 0.9673 positrons per decay [24]. The product between absorbed dose per positron and positron per decay returns de S-value (absorbed dose per decay). The number of particle histories simulated (NPS) by MCNP6 was set to 2.0E+07 in all the simulated cases.

## 3. RESULTS AND DISCUSSION

Figure 1 shows an $^{18}$F-FES/PET rendered image of a female Swiss mouse, 60min after injection. A median 3D filter was applied.

**Figure 1:** *$^{18}$F-FES /PET image obtained with AMIDE software for a female Swiss mouse, 60 min after radiopharmaceutical injection. The main uptake organs are indicated with arrows.*

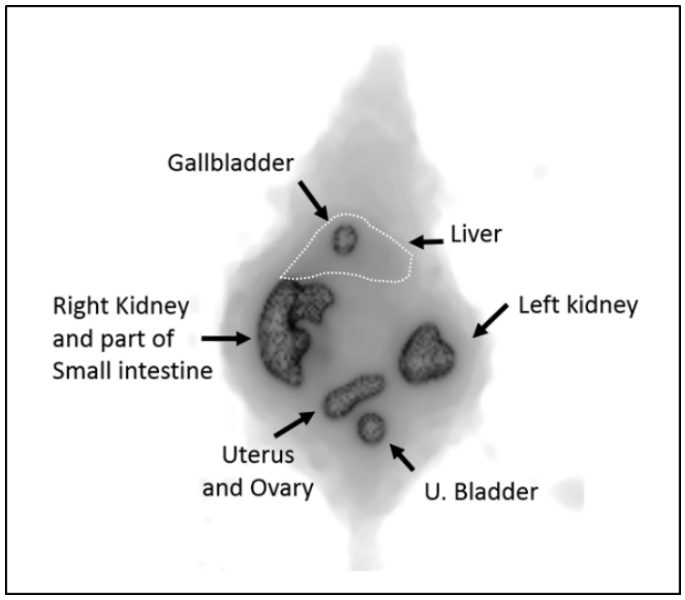

Qualitative analysis of the PET image (Figure 1) indicates a radiopharmaceutical metabolic behavior in accordance with literature: liver metabolism, urinary and bile excretion and high reabsorption of metabolites in small intestine [5]. Liver uptake is lower at this time (60 min after injection), but its contour is still visible. A high level of uptake was observed in the gall bladder.

The high reabsorption of metabolites in the small intestine is very evident in Figure 1, indicating that lower injected activity could be used in future images. Low background uptake was observed for most of the organs. Uterus and ovary presented significant uptake, indicating the $^{18}$F-FES affinity to estrogen receptors expressing tissues.

The $^{18}$F-FES *ex vivo* biodistribution results were presented in Figure 2. Data are expressed as percentage of injected dose per gram of tissue (%ID/g). Blood $^{18}$F-FES concentration significantly decreased from 1.36 %ID/g at 5 min to 0.08 % ID/g at 180 min after injection. High liver uptake at 5 min indicates the hepatic metabolism of $^{18}$F-FES, while high small intestine uptake indicates the metabolites reabsorption in this intestine portion, as described in literature [5]. The uptake in the uterus indicates the $^{18}$F-FES affinity with tissues expressing estrogen receptors.

**Figure 2:** *$^{18}$F-FES biodistribution in female Swiss mice. Data were obtained in five time points: 5, 30, 60, 120 and 180 minutes.*

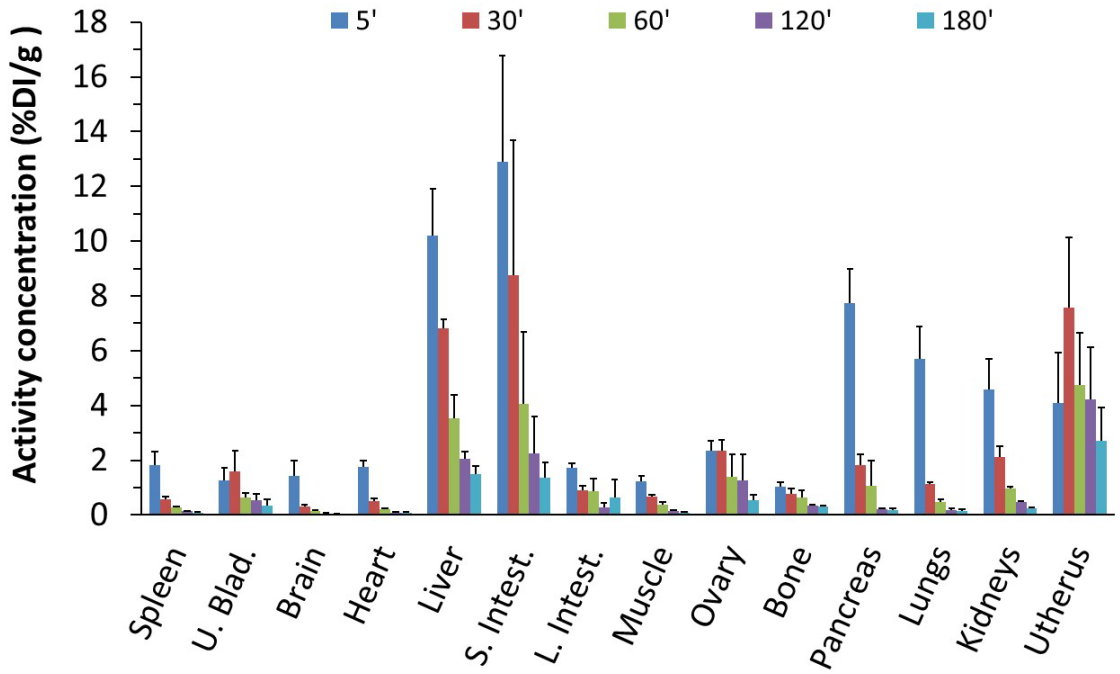

The $^{18}$F-FES is an estrogen receptor (ER) binding radiopharmaceutical. There are two subtypes of estrogen receptors: ERα and ERβ. According to Dahlman-Wright et al., (2006), in a female organism ERα is expressed predominantly in mammary gland, uterus, ovary, bone, liver, and adipose tissue. On the other hand, ERβ is more expressed in urinary bladder, ovary, colon, adipose tissue, and immune system. Both subtypes are significantly expressed in the cardiovascular and central nervous systems [25]. Most of the organs evaluated in the ex vivo biodistribution study show a "fast wash in" behavior (less than 5 minutes) and a continuous exponential decrease of the activity concentration in the remaining time points evaluated. However, for urinary bladder, uterus and ovary, the activity concentration for the 30 minutes time point were equal or even higher than 5 minutes point. Despite that urinary bladder, uterus and ovary organs were mentioned as organs of high ER expression, the receptors could not be so readily available for binding as the other organs due to specific vasculature and microcirculation characteristics. Another option that may explain this difference in biokinetic behavior is that $^{18}$F-FES have different affinities for ERα and ERβ. In fact $^{18}$F-FES affinity for ERα is 6.3 times higher than ERβ [26]. In this case, the receptor with less affinity (ERβ) could be more expressed in urinary bladder, uterus and ovary, or these organs may have high concentration of both receptors. In both cases, these organs will need more time to be saturated with $^{18}$F-FES. As far as we know, these hypotheses still need to be proved and should be evaluated in the future. Possibly, with a higher injected activity, these ERβ could be saturated earlier. However, that could not be assessed in this work.

The Time-Integrated Activities (Ã) calculated for 1.0 MBq of $^{18}$F-FES injected activity for the different organs and tissues of the FM_BRA mice phantom were presented in Table 1.In the image of Figure 1, low uptake was observed in the group of remaining organs. However, if the quotient Ã/mass of the organ was taken into account, it can be noted that the remaining organs show the higher Ã/mass value: 542 MBq.s.g$^{-1}$. Other organs that show clearly more uptake in Figure 1, like uterus, liver, and small intestine presented lower Ã/mass than "remaining organs": 354 MBq.s.g$^{-1}$, 294 MBq.s.g$^{-1}$ and 246 MBq.s.g$^{-1}$, respectively. Thus, the conservative approach adopted in this study, i.e., considering that all decays will occur inside the animal, resulted in overestimated values of Ã in remaining organs like eyes, gallbladder, salivary glands, spinal cord and stomach. That overestimation was reflected in the dosimetry results. However, in absence of data quantifying the

amount of decays that not occur inside the animal because renal and/or fecal excretion, the conservative data is still useful.

**Table 1:** Time-Integrated Activities of $^{18}$F-FES calculated for different organs of the *ex vivo* study and for the remaining organs of the FM_BRA mice model.

| ***Ex vivo* Organs** | **Mass [g]** | **Ã (Mbq.s)** |
|---|---|---|
| Bone | 0.873 | 35.97 |
| Brain | 0.382 | 7.91 |
| Heart | 0.270 | 7.78 |
| Intestine | 1.857 | 457.62 |
| Kidneys | 0.282 | 27.63 |
| Liver | 1.740 | 512.61 |
| Lung | 0.161 | 12.67 |
| Muscle | 5.197 | 160.56 |
| Ovary | 0.014 | 1.08 |
| Pancreas | 0.155 | 18.93 |
| Spleen | 0.079 | 2.62 |
| Urinary Bladder | 0.026 | 1.77 |
| Uterus | 0.125 | 44.27 |
| Remaining Organs * | 15.151 | 8210.53 |

| **Remaining Organs** | **Mass [g]** | **Norm** | **Ã (MBq.s)** |
|---|---|---|---|
| Non Segmented Soft Tissues | 14.556 | 0.9607 | 7888.2 |
| Gallbladder | 0.060 | 0.0040 | 32.6 |
| Stomach | 0.158 | 0.0104 | 85.7 |
| Salivary Glands | 0.194 | 0.0128 | 105.3 |
| Thyroid | 0.085 | 0.0056 | 46.0 |
| Spinal Chord | 0.091 | 0.0060 | 49.4 |
| Eyes | 0.006 | 0.0004 | 3.4 |
| **Total** | 15.151 | 1.0000 | 8210.5 |

* - $\tilde{A}_{\text{remaining organs}} = 9502$ MBq.s - $(\sum \tilde{A}_{\text{ex vivo organs}})$

$^{18}$F-FES preliminary dosimetry estimates for the female mice, based in Time-Integrated Activities values presented in Table 1, were presented in Table 2. Non-segmented soft tissues (NSST), eyes, gallbladder, salivary glands, spinal cord and stomach presented high dose coefficients per unit of injected activity, as expected, because of the conservative approach adopted in this work.

Among the organs measured in the *ex vivo* biodistribution, and therefore not affected by the "remaining organs" compartment overestimations, higher absorbed doses were found in uterus, liver, intestine, ovary and urinary bladder. Uterus, ovary, urinary bladder and liver are organs with high concentration of estrogen receptors [25]. High absorbed dose values for liver and intestine may be explained due to the $^{18}$F-FES hepatic metabolism and the high reabsorption of metabolites in the small

intestine. Bone, heart and brain, although mentioned as organs with significant expression of estrogen receptors [25], presented low values of uptake (Table 1) and lower absorbed dose levels (Table 2). That is an unexpected outcome that should be evaluated in future works.

**Table 2:** $^{18}$F-FES preliminary dosimetry estimates for the female mice

| Target organ | Absorbed Dose per Injected Activity (mGy/MBq) | Target organ | Absorbed Dose per Injected Activity (mGy/MBq) |
|---|---|---|---|
| Stomach | 22.1 | Ovary | 10.4 |
| Thyroid | 22.1 | Urinary Bladder | 9.7 |
| Gallbladder | 21.5 | Pancreas | 9.3 |
| Salivary Glands | 21.0 | Kidneys | 8.1 |
| NSST | 20.4 | Spleen | 7.0 |
| Eyes | 18.9 | Lungs | 7.0 |
| Uterus | 17.3 | Muscle | 5.0 |
| Spinal Cord | 16.2 | Bone | 4.8 |
| Liver | 14.3 | Heart | 3.5 |
| Intestine | 13.4 | Brain | 3.0 |

## 4. CONCLUSION

A preliminary dosimetry data set based on a voxelized female mice model was obtained for $^{18}$F-FES. This is the first time that mice dosimetry for $^{18}$F-FES is presented. In our dosimetry study, we adopted a highly conservative hypothesis. We considered that all decays from the injected activity would occur in the animal. This approach lead to overestimated values in eyes, gallbladder, salivary glands, spinal cord and stomach. Those are the organs not evaluated in *ex vivo* biodistribution. Among the organs targeted *ex vivo* biodistribution, uterus, liver, intestine and ovary presented the higher absorbed dose values. These findings were in accordance with the microPET images.

In spite of some overestimations, the dosimetric data generated is still relevant to a first estimative of animal radiation dose in preclinical investigations and to avoid high animal absorbed dose that may interfere with the experiments.

The study is not finished yet and some improvements are required to the female mouse model. Future biodistribution studies should focus in the evaluations of the optimal injected dose as well as in the quantification of the activity in intestine contents and in the urine, for obtaining urinary and fecal excretion models. This could improve the dosimetry estimations and the image quality.

## ACKNOWLEDGMENT

Authors thanks CDTN/CNEN, PIBIC/CNPq, FAPEMIG and UFMG for supporting this work.

## REFERENCES

[1] INCA – Instituto Nacional do Câncer José Alencar Gomes da Silva. Estimativa 2014: **Incidência de Câncer no Brasil.** Rio de Janeiro: INCA, 2014.

[2] FLANAGAN, F. L et al., PET in Breast Cancer. **Semin Nucl Med**, v. 28, p. 290-302, 1998.

[3] LINDEN, H. M. L et DEHDASHTI, F. Novel Methods and Tracers for Breast Cancer Imaging, **Semin. Nuc. Med.** v. 43, n. 4, p. 324-329 2013.

[4] ALAM, I. S. et al., Radiopharmaceuticals as probes to characterize tumor tissue, **Eur. J. Nuc. Med. Mol. Imag.** v. 42, n. 4, p. 537-561, 2015.

[5] SUDARARAJAN, L. et al., 18F-Fluoroestradiol, **Semin Nucl Med**, v. 37, n. 6, p. 470-476, 2007.

[6] ORDINAS, H. E. et al., PET imaging to non-invasively study immune activation leading to antitumor responses with a 4-1BB agonistic antibody, **J. Immunother. Cancer**, v. 1, n. 14, p. 1-11, 2013.

[7] WANG, Y. et al., [18F]DPA-714 PET Imaging of AMD3100 Treatment in a Mouse Model of Stroke, **Mol. Pharm.**, v. 11, p. 3463-3470, 2014.

[8] VAHLE, A.K. et al., Multimodal imaging analysis of an orthotopic head and neck cancer mouse model and application of anti-CD137 tumor immune therapy, **Head Neck**, v. 38, n. 4, p. 542-529, 2016.

[9] STELLAS, D. et al., Therapeutic Effects of an Anti-Myc Drug on Mouse Pancreatic Cancer, **J. Natl. Cancer Inst.**, v. 106, n. 12, p. 1-8, 2014.

[10] REX, K. et al., Evaluation of the antitumor effects of rilotumumab by PET imaging in a U-87 MG mouse xenograft model, **Nucl. Med. Biol.**, v. 40, n. 4, p. 458-463,2013.

[11] POLLOK, K.,E. et al., In Vivo Measurements of Tumor Metabolism and Growth after Administration of Enzastaurin Using Small Animal FDG Positron Emission Tomography, **J Oncol**, v. 2009, Article ID 596560, 8 pages, doi:10.1155/2009/596560, 2009

[12] S. Hu et al., Longitudinal PET Imaging of Doxorubicin-Induced Cell Death with 18F-Annexin V., **Mol Imaging Biol,** v. 14, p. 762-770, 2012

[13] DUNCAN K. et al., 18F-FDG-PET/CT imaging in an IL-6- and MYC-driven mouse model of human multiple myeloma affords objective evaluation of plasma cell tumor progression and therapeutic response to the proteasome inhibitor ixazomib, **Blood Cancer J**, v. 3, p. 1-12, 2013.

[14] WANG G. J. et CAI L.., Induction of Cell-Proliferation Hormesis and Cell-Survival Adaptive Response in Mouse Hematopoietic Cells by Whole-Body Low-Dose Radiation, **Toxicol. Sci.**, v. 53, p. 369–376, 2000.

[15] YANEZAWA M, Induction of radio-resistance by low dose X-irradiation **Yakugaku Zasshi**, v. 126, n. 10, p. 833–840, 2006.

[16] MENDES, B. M. et al., Development of a mouse computational model for MCNPx based on Digimouse® images and dosimetric assays, **Braz. J. Pharm. Sci.**, 2017; v. 53, n. 1, 2017

[17] KINASE, S. et al., Computer Simulations for Internal Dosimetry Using Voxel Models, **Radiat. Prot. Dosim,** v. 146, n. 1-3, p. 191–194, 2011.

[18] BISPO, A.C.A. et al., Development of a Female Mouse Computational Model Based on CT Images for Dosimetric Assays. In: http://repositorio.ipen.br/bitstream/handle/123456789/32876/28598.pdf?sequence=1&isAllowed=y; Accessed: 2022, July.

[19] BISPO, A.C.A. et al., Synthesis and characterization of the radiopharmaceutical [$^{18}$F]fluoroestradiol, **Braz. J. Radiat. Sci.**, v. 09, n. 01A, p. 01-11, 2021

[20] LOENING, A. M. and GAMBHIR, S. S. AMIDE: A Free Software Tool for Multimodality Medical Image Analysis. **Mol. Imaging**, v. 2, n. 3, p. 131–137, 2003

[21] BOLCH, W. E. et al., MIRD pamphlet no. 21: a generalized schema for radiopharmaceutical dosimetry-standardization of nomenclature, **J Nucl MED**, v. 50, p. 477-84, 2009.

[22] GOORLEY, J. T. et al., **MCNP6 User's Manual, Version 1.0**, LA-CP-13-00634, Los Alamos National Laboratory, no. LA-CP-13-00634. p. 765, 2013.

[23] ICRP, ICRP Publication 110: Adult Reference Computational Phantoms, **Ann. ICRP**, v. 39, n. 2, pp. 47–70, 2009.

[24] ICRP, ICRP Publication 107: Nuclear decay data for dosimetric calculations, **Ann. ICRP**, vol. 38, no. 3, pp. 7–96, 2008.

[25] DAHLMAN-WRIGHT, K et al., International Union of Pharmacology. LXIV. Estrogen Receptors. **Pharmacol. Rev.** vol.58, pp. 773–781, 2006.

[26] NHI. National Cancer Institute. FES Documentation Page. [$^{18}$F] FES Investigator's Brochure. In: https://imaging.cancer.gov/programs_resources/cancer-tracer-synthesis-resources/docs/fes_ib_pdf.pdf. Accessed: 2022, July.